PERIODICA POLYTECHNICA SER. CHEM. ENG. VOL. 41, NO. 1, PP. 57–72 (1997)

# MULTICOMPONENT DIFFUSION AND REACTION IN COMPOSITE CATALYSTS - A MONTE-CARLO AND DUSTY-GAS MODEL APPROACH APPLIED TO THE METHANOL-TO-OLEFIN SYNTHESIS IN ZEOLITES[1]

Abdul R. GARAYHI and Frerich J. KEIL

Department of Chemical Engineering
Technische Universität Hamburg-Harburg
Eißendorferstraße 38, D-21071 Hamburg, Germany
Fax : +49-40-7718-2573
E-mail : keil@tu-harburg.d400.de

Received: Apr. 1, 1997

## Abstract

A model of the description of reaction and mass transport within composite catalysts by Ruckenstein was improved by taking a volume change during the reaction into account, and by describing the internal fluxes by the Dusty-Gas Model. A new numerically improved notation of the Dusty-Gas-Model equations was investigated. The new model is used for describing the Methanol-To-Olefin synthesis in zeolite catalysts. The diffusivities in zeolite particles were obtained by a Monte-Carlo approach. The new model offers an improved description of experimental data.

*Keywords:* composite catalysts, dusty-gas model, volume change, zeolites, methanol-to-olefin synthesis.

## 1. Introduction

Composite catalysts consist of small catalytically active particles that are embedded in a nearly inert matrix. They are in industrial use as they combine good catalytic properties of the active material (e. g. zeolites) with good mass-transfer properties of the matrix material. The catalysts can be made more abrasion resistant. Even if only small active particles can be manufactured, composite catalysts of any size can be produced.

For example composite catalysts are employed in Methanol-To-Olefin (MTO) synthesis. They consist of zeolites embedded into an amorphous silica-alumina matrix. During MTO synthesis methanol is converted into olefins and paraffins in fluidized-bed reactors.

In order to describe this reaction reliably it was necessary to extend an earlier model proposed by Ruckenstein in three different respects:

---

[1] The authors are grateful to the Max-Buchner-Stiftung (Grant No. 1772) and to the Fonds der Chemischen Industrie

- A volume change during the reaction has to be taken into account.
- Any common chemical kinetics should be employable.
- The fluxes within the amorphous matrix are described by the Dusty-Gas Model. This model allows to include multicomponent effects. A new, numerically more stable description of the system of model equations was developed.

## 2. Stefan–Maxwell Diffusion and the Dusty-Gas Model

According to the Dusty-Gas Model the flux is divided into three parts:

$$\mathbf{j} = \mathbf{j}^D + \mathbf{j}^S + \mathbf{j}^V, \tag{1}$$

where ($\mathbf{j}^D$ ) represents the part resulting from Knudsen diffusion and molecular diffusion. This term will be discussed below. The resistances of this kind of diffusion leads to:

$$\mathbf{j}^S = -\mathbf{D}^S \frac{d\mathbf{c}}{dr} \tag{2}$$

with the matrix of surface diffusivities like this:

$$\mathbf{D}^S = \begin{cases} D_i{}^S| & i = j \\ 0 & | \quad i \neq j \\ , & \end{cases} \tag{3}$$

KRISHNA (1993) has developed a model which makes it possible to include the interactions of different species adsorbed on the surface. From a mathematical point of view it is equivalent to the Stefan–Maxwell approach for bulk diffusion given below. Interactions of adsorbed species are taken into account by means of a counter sorption diffusivity. In the example presented in this paper the surface flux is neglected, because the species involved rarely adsorb.

Additionally to the diffusive fluxes there is a viscous flux due to a pressure gradient. In cylindrical pores, the viscous flux can be estimated by Hagen–Poisseuille's Law:

$$\mathbf{j}^V = -\mathbf{c} \frac{r_p^2}{8\eta} \frac{dp}{dr}. \tag{4}$$

Assuming ideal-gas behaviour, one finds:

$$\mathbf{j}^V = -\mathbf{c} RT \frac{r_p^2}{8\eta} \frac{dc_t}{dr}. \tag{5}$$

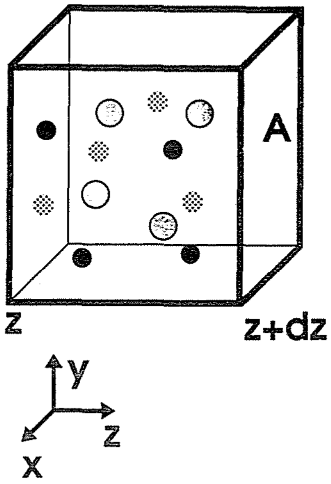

*Fig. 1.* A control volume with particles of different species

### 2.1 The Diffusive Flux

Diffusion is the transport of particles (atoms or molecules) due to a concentration gradient. First, a model for the multicomponent diffusion, the Stefan–Maxwell approach, in a free space will be shortly presented.

Some particles can be regarded as being within a control volume to be $dz$ in length and a cross-section $A$ perpendicular to the $z$-axis (*Fig. 1*). The particles shall be uniformly distributed along the $x$- and $y$- direction. The resulting one-dimensional equations can straightforwardly be extended to a three-dimensional case. The forces that have an effect on the particles of a species $i$ in this control volume are the counteracting forces to the forces the particles would exert on walls of the control volume

$$-dF_i = p_i(z + dz) \cdot A - p_i(z) \cdot A. \tag{6}$$

Expanding the partial pressure into a first-order Taylor series, one finds:

$$p_i(z + dz) \approx p_i(z) + \frac{dp_i}{dz} \cdot dz. \tag{7}$$

Combining these equations leads to:

$$-dF_i \approx \frac{dp_i}{dz} \cdot dz \cdot A. \tag{8}$$

If an infinitely small control volume is taken, the average force on the particles of species $i$ is given by:

$$-\frac{dF_i}{dV} = -\frac{dF_i}{dz \cdot A} = -\frac{dp_i}{dz}. \tag{9}$$

The force is exerted only by momentum exchange with particles of other species. (Momentum exchange between particles of the same species does not change the average values). The average rate of momentum exchange is given by the collision rate, $s$, and the average momentum exchanged during a single collision, $\Delta \wp_{ij}$:

$$\frac{\Delta \wp_i}{\Delta t} = \sum_{j=1}^{N} \Delta \wp_{ij} \cdot s. \tag{10}$$

The momentum exchanged during a collision can be regarded as being proportional to the relative velocity of the colliding particles. It should be noticed that this assumption does not necessarily include a hard-sphere potential for the molecules:

$$\Delta \wp_{ij} = c_{\Delta \wp_{ij}} \cdot (u_i - u_j). \tag{11}$$

The collision rate is proportional to the number of particles of the colliding species. The proportionality factor, $c_s$, is a function of the system pressure (and thereby of the total number of particles) and temperature and is specific relating to the substances. It is independent of the volume fractions of the colliding species:

$$s = c_s \cdot n_i \cdot n_j. \tag{12}$$

Combining *Eqs.* (9–12) and assuming ideal-gas behaviour yields:

$$\frac{\Delta \wp_i}{\Delta t} = \frac{p \cdot n_t \cdot dV}{k_B \cdot T} \sum_{j=1}^{N} c_s \cdot c_{\Delta \wp_{ij}} \cdot x_i \cdot x_j \cdot (u_i - u_j) \tag{13}$$

or

$$\frac{\Delta \wp_i}{\Delta t \cdot dV} = p \cdot \sum_{j=1}^{N} \frac{c_s \cdot c_{\Delta \wp_{ij}} \cdot n_t}{k_B \cdot T} \cdot x_i \cdot x_j \cdot (u_i - u_j). \tag{14}$$

The first term of the sum is combined to the 'diffusivity', $D_{ij}$.

Chapman and Enskog have (independently of each other) deduced the diffusivity from the Boltzmann equation (CHAPMAN, 1917; BIRD, 1994):

$$D_{ij} = \frac{\frac{3}{16}\sqrt{\frac{2\pi k_B T}{m_r}}}{\left(\frac{m_r}{2k_B T}\right)^3 \int_0^\infty u_r^5 \sigma_M \exp\left\{-\frac{m_r u_r^2}{2k_B T}\right\} du_r} \tag{15}$$

with the reduced mass

$$m_r = \frac{m_i \cdot m_j}{m_i + m_j} \tag{16}$$

and the scattering cross-section:

$$\sigma_M = 2\pi \int_0^\pi \sigma(1 - \cos\chi)\sin\chi d\chi. \tag{17}$$

If a hard-shere potential is assumed, these equations simplify to:

$$D_{ij} = \frac{3 \cdot \sqrt{\frac{2\pi k_B T}{M_{ij}}}}{16 n_t \sigma_{T12}}. \tag{18}$$

Combining *Eqs.* (9) and (14), one finds:

$$-\frac{dp_i}{dz} = p \cdot \sum_{j=1}^{N} \frac{x_i \cdot x_j \cdot (u_i - u_j)}{D_{ij}}. \tag{19}$$

Using a three-dimensional approach, one would find a similar result:

$$-\frac{\nabla p_i}{p} = \sum_{j=1}^{n} \frac{x_i \cdot x_j \cdot (\mathbf{u}_i - \mathbf{u}_j)}{D_{ij}}. \tag{20}$$

*Eq.* (20) can be written in terms of the diffusive fluxes, $\mathbf{j}_i = c_i \cdot \mathbf{u}_i$. One finds:

$$c_t \cdot \frac{\nabla p_i}{p} = \sum_{j=1}^{N} \frac{x_i \mathbf{j}_j}{D_{ij}} - \frac{x_j \mathbf{j}_i}{D_{ij}} \tag{21}$$

$$= \sum_{\substack{k=1 \\ k \neq i}}^{N} \frac{x_i \mathbf{j}_j}{D_{ij}} - \sum_{\substack{k=1 \\ k \neq i}}^{N} \frac{x_j \mathbf{j}_i}{D_{ij}}. \tag{22}$$

There is no net flux, so

$$\mathbf{j}_i = -\sum_{\substack{l=1 \\ l \neq i}}^{N} \mathbf{j}_l. \tag{23}$$

*Eq.* (22) becomes:

$$c_t \cdot \frac{\nabla p_i}{p} = \sum_{j=1}^{N} \frac{x_i \mathbf{j}_j}{D_{ij}} + \frac{x_j}{D_{ij}} \left( \sum_{\substack{l=1 \\ l \neq i}}^{N} \mathbf{j}_l \right) \tag{24}$$

$$\nabla c_i = \sum_{\substack{j=1\\ j\neq i}}^{N} \left( \frac{x_i}{D_{ij}} + \sum_{\substack{l=1\\ l\neq i}}^{N} \frac{x_l}{D_{il}} \right) \mathbf{j}_j . \tag{25}$$

This equation is numerically more stable than the common expression

$$c_t \cdot \frac{\nabla p_i}{p} = \nabla c = -\left( \frac{x_i}{D_{in}} + \sum_{\substack{l=1\\ l\neq i}}^{N} \frac{x_l}{D_{il}} \right) \mathbf{j}_i + \sum_{\substack{j=1\\ j\neq i}}^{N-1} -x_i \left( \frac{1}{D_{ij}} - \frac{1}{D_{iN}} \right) \mathbf{j}_j , \tag{26}$$

which may be found by substituting $\mathbf{j}_N$ rather than $\mathbf{j}_i$.

If diffusion does not take place in free space but in porous media, additional interactions with the walls are to be taken into account. This can be done by introducing the wall as the species $N+1$, consisting of heavy particles ('dust'). The following assumptions are made:

- The wall particles are much heavier than the gas particles.
- The particles are kept fixed in their positions by external forces. Their flux is zero, $\mathbf{j}_{N+1} = 0$. The origin of the forces is not considered.
- The particles are uniformly distributed in space.

It should be noticed that the actual geometric structure can only be introduced indirectly. This has been done in several ways (see for example FENG, 1972; RIECKMANN and KEIL, 1997). In principle, the Dusty-Gas-Model can be adopted to any internal geometry of the porous media.

In practical implementation, particle–wall interactions are taken into account by means of the Knudsen diffusivity $D_i^K$. From the kinetic gas theory one finds:

$$D_i^K = \frac{2}{3} r_P \sqrt{\frac{8RT}{\pi M_i}} . \tag{27}$$

The fraction of dust particles, $x_{N+1}$, is thereby set to unity. *Eq.* (25) becomes:

$$\nabla \mathbf{c}_i = \sum_{\substack{j=1\\ j\neq i}}^{N} \left( \frac{x_i}{D_{ij}} + \sum_{\substack{l=1\\ l\neq i}}^{N} \frac{x_l}{D_{il}} + \frac{1}{D_i^K} \right) \mathbf{j}_j \tag{28}$$

or in matrix notation

$$\nabla \mathbf{c} = -\mathbf{D} \cdot \mathbf{j} \tag{29}$$

with the $N \times N$ matrix

$$-\mathbf{D} = \begin{cases} \frac{x_i}{D_{ij}} + \sum_{\substack{l=1\\ l\neq i}}^{N} \frac{x_l}{D_{il}} + \frac{1}{D_i^K} | & i \neq j \\ 0 \qquad\qquad | & i = j \end{cases} . \tag{30}$$

In porous media the area available for mass transport is smaller than in free space. This leads to a smaller effective flux. A correction is possible by introducing the porosity, $\epsilon$, and the tortuosity, $\tau$:

$$\mathbf{j}_{eff} = \frac{\epsilon}{\tau}\mathbf{j}. \tag{31}$$

For practical purposes, an effective diffusivity is introduced to describe the diffusive fluxes:

$$D_{eff} = \frac{\epsilon}{\tau}D. \tag{32}$$

## 3. A Model for Composite Catalyst Particles

According to RUCKENSTEIN (1970), one can assume that reaction and diffusion in the two phases, the catalytically active and the matrix phase, can be treated independently. The fluxes and reaction rates in both phases are added:

$$\mathbf{j}_t = (1-\zeta)\cdot\mathbf{j}_m + \zeta\cdot\mathbf{j}_a \tag{33}$$

and

$$R_t = (1-\zeta)\cdot R_m + \zeta\cdot R_a. \tag{34}$$

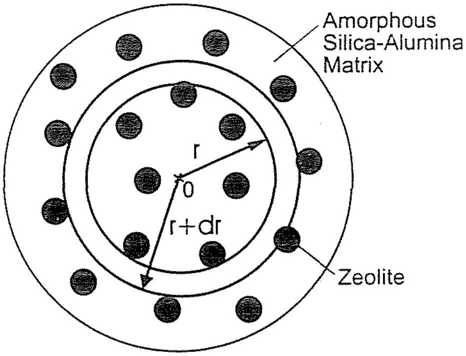

*Fig. 2.* Schematic view of a composite catalyst particle

The material balance over a spherical shell of the pellet (*Fig. 2*) under steady-state conditions gives:

$$\begin{aligned}0 =&(1-\zeta)\cdot \mathbf{j}_m(r)\cdot A(r) - (1-\zeta)\cdot \mathbf{j}_m(r+dr)\cdot A(r+dr)\\ &+\zeta\cdot \mathbf{j}_a(r)\cdot A(r) - \zeta\cdot \mathbf{j}_a(r+dr)\cdot A(r+dr) + (1-\zeta)\cdot\sum_{i=1}^{n_r}\nu_i\cdot R_m(r)\cdot dV\\ &+\zeta\cdot\sum_{i=1}^{n_r}\nu_i\cdot R_a(r)\cdot dV.\end{aligned} \tag{35}$$

The multicomponent flux within the amorphous matrix can be described by the Dusty-Gas Model. In the present example there is a configurational diffusion inside the active particles (zeolites). The effective diffusivities within the zeolites are found by Monte-Carlo simulations and also include the viscous flux. The fluxes can be expressed as:

$$\mathbf{j}_a = -\mathbf{D}_{eff}\cdot\frac{d\mathbf{c}}{dr}, \tag{36}$$

where ($\mathbf{D}_{eff}$) is similar to ($\mathbf{D}^S$) in *Eq.* (3).

By making use of relation (36) the mass balance (*Eq.* (35)) can be converted by expanding the fluxes, $\mathbf{j}$, and the area, $A$, into the first two terms of Taylor series':

$$\mathbf{j}(r+dr) = \mathbf{j}(r) + \frac{d\mathbf{j}}{dr}\cdot dr, \tag{37}$$

$$A(r+dr) = A(r) + \frac{dA}{dr}\cdot dr, \tag{38}$$

The differential mass balance for an arbitrary component, $i$, and $n_r$ reactions becomes:

$$\begin{aligned}0 =&(1-\zeta)\Bigg\{(\mathbf{j}_m^D+\mathbf{j}_m^S+\mathbf{j}_m^V)_r\cdot A(r)\\ &-\left[(\mathbf{j}_m^D+\mathbf{j}_m^S+\mathbf{j}_m^V)_r + \frac{d(\mathbf{j}_m^D+\mathbf{j}_m^S+\mathbf{j}_m^V)}{dr}\cdot dr\right]\cdot\left[A(r)+\frac{dA}{dr}\cdot dr\right]\\ &+\sum_{r=1}^{n_r}\nu_{jr}\cdot R_{m,r}\cdot A(r)\cdot dr\Bigg\}\\ &+\zeta\Bigg\{\mathbf{j}_a^D\cdot A(r) - \left[\mathbf{j}_a^D + \frac{d\mathbf{j}_a^D}{dr}\cdot dr\right]\cdot\left[A(r)+\frac{dA}{dr}\cdot dr\right]\\ &+\sum_{r=1}^{n_r}\nu_{jr}\cdot R_{a,r}\cdot A(r)\cdot dr\Bigg\}\end{aligned} \tag{39}$$

or

$$0 = (1-\zeta)\Bigg\{ -(\mathbf{j}_m^D + \mathbf{j}_m^S + \mathbf{j}_m^V)_r \cdot \frac{dA}{dr} \cdot \frac{1}{A(r)} - \frac{d(\mathbf{j}_m^D + \mathbf{j}_m^S + \mathbf{j}_m^V)}{dr} + \sum_{r=1}^{n_r} \nu_{jr} \cdot R_{m,r} \Bigg\} + \zeta \Bigg\{ -\mathbf{j}_a^D \cdot \frac{dA}{dr} \cdot \frac{1}{A(r)} - \frac{d\mathbf{j}_a^D}{dr} + \sum_{r=1}^{n_r} \nu_{jr} \cdot R_{a,r} \Bigg\}. \quad (40)$$

The rate of reaction inside the active component, $R_a$, can be calculated by means of an effectiveness factor of the active particles, $\varphi^a$, and the intrinsic rate of reaction, $R_a^{int}$:

$$R_a = \varphi^a \cdot R_a^{int}. \quad (41)$$

Within the matrix phase there is no further diffusion limitation, all components have unlimited access to the active sites. So *Eq.* (40) becomes:

$$\begin{aligned} 0 = &\left[(1-\zeta)\left\{\mathbf{D}^{-1} + \mathbf{D}^S + RT\frac{r_P^2}{8\eta}\mathbf{c}\mathbf{e}^T\right\} + \zeta\mathbf{D}_{eff}^a\right]\frac{d^2\mathbf{c}}{dr^2} \\ &+ \left[(1-\zeta)\left\{\frac{2}{r}\left(\mathbf{D}^{-1} + \mathbf{D}^S + RT\frac{r_P^2}{8\eta}\mathbf{c}\mathbf{e}^T\right) + \frac{d\mathbf{D}^{-1}}{dr} + RT\frac{r_p^2}{8\eta}\frac{d\mathbf{c}}{dr}\mathbf{e}^T\right\}\right. \\ &\left. + \frac{2}{r}\zeta\mathbf{D}_{eff}^a\right]\frac{d\mathbf{c}}{dr} + (1-\zeta)\sum_{i_r=1}^{n_r} \nu_{i_r} R_{m,i_r} + \zeta \sum_{i_r=1}^{n_r} \nu_{i_r}\varphi^a R_{a,i_r}. \end{aligned} \quad (42)$$

The corresponding boundary values are:

$$\mathbf{c}(R_0) = \mathbf{c}_S \quad (43)$$

and

$$\left.\frac{d\mathbf{c}}{dr}\right|_{r=0} = 0. \quad (44)$$

Usually, the concentrations at the surface, $\mathbf{c}_S$, are unknown. In addition, the concentrations depend on the external mass-transfer resistance. Therefore, the first boundary value is replaced by the equation:

$$\mathbf{k}_S(\mathbf{c}_S - \mathbf{c}_b) = (1-\zeta)\mathbf{j}_m\big|_{r=R_0} + \zeta\mathbf{j}_a\big|_{r=R_0}. \quad (45)$$

### *3.1 Data and Algorithms*

For an exact solution, the effectiveness factor, $\varphi^a$, can be calculated from a boundary-value system similar to *Eqs.* (42–45) with $\zeta = 1$. As the calculation of the exact values would be very time-consuming, in this work the effectiveness factor is calculated approximately. For the approximation the factor is calculated as in the case of a first-order reaction without any change in volume. A first-order reaction from the scheme is taken as a key reaction:

$$\varphi^a = \frac{3}{\Phi_a}\left[\frac{1}{\tanh(\Phi_a)} - \frac{1}{\Phi_a}\right] \tag{46}$$

with the Thiele–modulus of the active particles

$$\Phi_a = r_0 \cdot \sqrt{\frac{k_a}{D^a}}. \tag{47}$$

The diffusivities within the matrix phase are taken from the Fuller equation (FULLER et al., 1966):

$$D_{12} = \frac{10^{-3} T^{1.75} \sqrt{\frac{M_1 + M_2}{M_1 M_2}}}{p[(\sum \nu)_1^{\frac{1}{3}} + (\sum \nu)_2^{\frac{1}{3}}]^2}, \tag{48}$$

where $\nu$ are the diffusion volumes of chemical groups. Diffusivities within the zeolites were taken from Monte-Carlo simulations. They have been published previously (HINDERER and KEIL, 1994, 1996). The mass transfer coefficient, $k_s$, is difficult to determine at low Reynolds numbers (MARTIN, 1988). For the present examples the empirical correlation suggested by Kröger was used (BRAUER, 1971):

$$\frac{Sh}{Re Sc^{\frac{1}{3}}} \frac{1}{0.12 + \epsilon_r} = \frac{3.72}{Re^{\frac{2}{3}}} + \frac{1.06}{30 + Re^{\frac{1}{3}}}. \tag{49}$$

As an example the Methanol-To-Olefin synthesis (MTO synthesis) with a zeolite catalyst was chosen. The following reaction scheme was published previously (SCHOENFELDER et al., 1994):

$$A \xrightarrow{k_1} \frac{1}{2} B + W, \tag{50}$$

$$A + B \xrightarrow{k_2} C + W \tag{51}$$

$$A + C \xrightarrow{k_3} D + W, \tag{52}$$

$$B \xrightarrow{k_4} \frac{2}{3} E, \tag{53}$$

$$C \xrightarrow{k_4} E \tag{54}$$

$$D \xrightarrow{k_4} \frac{4}{3} E, \tag{55}$$

$$A \xrightarrow{k_5} \frac{3}{2} F + \frac{1}{2} W. \tag{56}$$

In this scheme some of the participating species are combined in the lumps A (methanol and dimethylether), E (paraffins) and F (decomposition products). The other components are abbreviated by B (ethene), C (propene), D (butene) and W (water). All kinetics were found to be first order in all reactants. In order to determine the rate constants, measurements were carried out in a Berty reactor. At 500 °C, the constants given in *Table 1* were found.

**Table 1**
Kinetic constants of the MTO Synthesis

| Temperature | 500°C |
|---|---|
| $k_1$ | $6.73 \cdot 10^{-3} \frac{\mathrm{m}^3}{\mathrm{s \cdot kg}}$ |
| $k_2$ | $3.42 \cdot 10^{-3} \frac{\mathrm{m}^6}{\mathrm{s \cdot kg \cdot mol}}$ |
| $k_3$ | $5.00 \cdot 10^{-4} \frac{\mathrm{m}^6}{\mathrm{s \cdot kg \cdot mol}}$ |
| $k_4$ | $2.09 \cdot 10^{-5} \frac{\mathrm{m}^3}{\mathrm{s \cdot kg}}$ |
| $k_5$ | $2.74 \cdot 10^{-4} \frac{\mathrm{m}^3}{\mathrm{s \cdot kg}}$ |

**Table 2**
Operating conditions used in the calculations

| Temperature | 500°C |
|---|---|
| Pressure | 1 bar |
| Bulk concentration | $\left[\frac{\mathrm{mol}}{\mathrm{m}^3}\right]$ |
| A | 0.252 |
| B | 0.538 |
| C | 1.708 |
| D | 1.192 |
| E | 0.227 |
| F | 0.151 |
| W | 11.698 |

The above system of ordinary differential equations (ODE system) was numerically solved using routines from the commercial package NAG (The Numerical Algorithms Group Ltd., Oxford, UK; Mark 17). A combined Powell-hybrid method (routine C05NDF) was used to find the roots of the algebraic equations resulting from the boundary conditions. Two different methods were employed to solve the boundary value problem, a shooting and matching technique (D02HAF) and a finite difference method (D02GAF).

Even in the simple case of just one irreversible reaction with just one reactant and using the Fickian law, it is impossible to calculate the concentrations in the pellet analytically if there is a change in volume during the reaction (THIELE, 1939).The effectiveness factors of some pellets were calculated as a function of pellet size and zeolite fraction.

## 4. Results and Discussion

Measured data of the effectiveness factor as function of particle size were published previously (HINDERER and KEIL, 1995). The same bulk concentrations and temperatures were used during these calculations. The calculated effectiveness factors as a function of particle size and zeolite fraction are shown in *Fig. 3.* Two different definitions of the effectiveness factor are found in the literature. Originally it was introduced as the ratio of the actual reaction rate to the reaction rate at surface conditions:

$$\varphi_S = \frac{r_{\text{exp}}}{r_{\text{int}}(c_S, T_S)}. \tag{57}$$

There is also a definition that uses the ratio of the actual reaction rate to the reaction rate under bulk conditions:

$$\varphi_b = \frac{r_{\text{exp}}}{r_{\text{int}}(\mathbf{c}_b, T_b)}. \tag{58}$$

Both values were calculated during this work. The external mass-transfer resistance appeared to be relatively low, so only small differences between the two effectiveness factors occurred.

For comparison, the effectiveness factors were also calculated by the formula of RUCKENSTEIN (1970). This equation allows to calculate the effectiveness factor in the case of a first-order reaction with a constant volume. The calculated effectiveness factor of a large particle is also shown in *Fig. 3.* The values of the effectiveness factor calculated using the model presented here are substantially lower than those obtained by the model by Ruckenstein, which does not take the volume change into account.

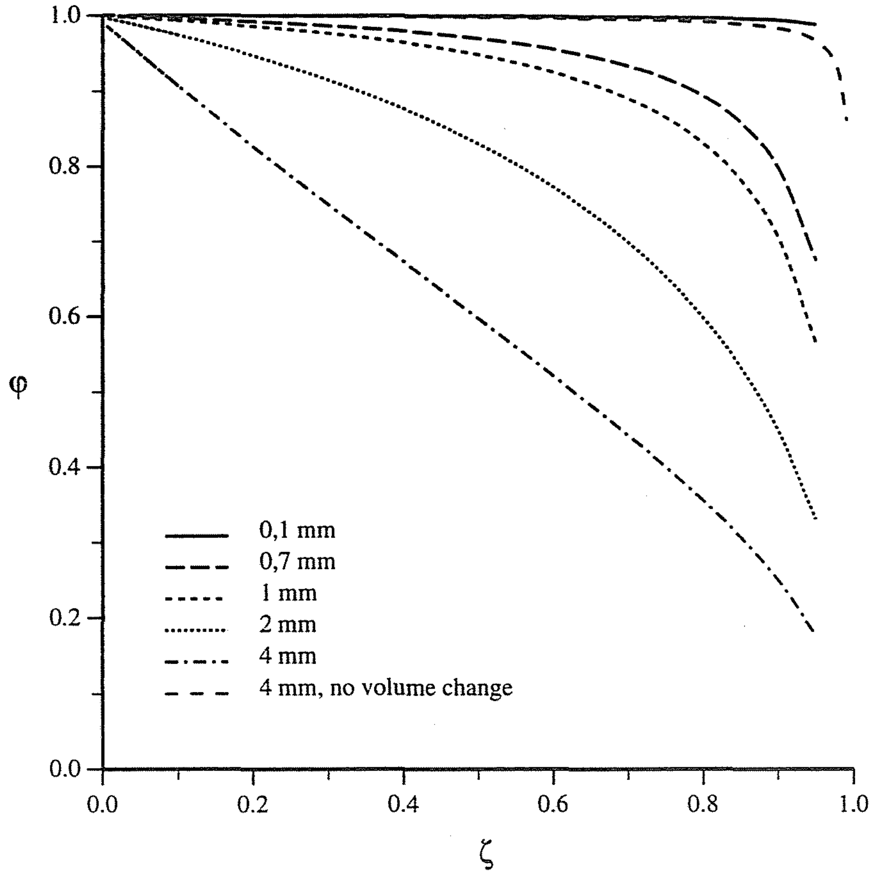

*Fig. 3.* Results of the calculations.

**Table 3**
Experimental and calculated effectiveness factors

| $d$[mm] | $\varphi_{exp}$ | $\varphi_{calc}$ |
|---|---|---|
| 0.7 | 1.00 | 1.00 |
| 1.2 | 0.98 | 0.99 |
| 2.0 | 0.96 | 0.97 |
| 4.0 | 0.78 | 0.91 |

The values calculated still differ from the measured results (*Table 3*). This effect vanishes, if the activity of the matrix phase is increased. Since amorphous alumina structures have a wide activity range (ESPIONZA et al., 1983), it is necessary to determine experimentally the activity of the matrix material used. Such a material was not available for the present authors.

The design of composite catalyst particles strives for an actual reaction rate as high as possible. According to the model presented in this work, this is the case for a particle consisting of pure zeolite material. Only if the diffusivities within the zeolite particles decrease substantially, a maximum at fractions less than one is found. In practice, there is another restriction: Soot is deposited inside the catalyst particles. This leads to a blocking of the pores. If the fraction of micropores is high, parts of the catalyst particles deactivate quickly. Macroporous material deactivates more slowly. From the results presented in this paper one can conclude that the diffusion resistance of small particles ($d \approx 1 \mu\mathrm{m}$) can be neglected even at high zeolite fractions. This enables to distinguish between different effects, e. g. pore blocking and diffusion limitation, while interpreting experimental results.

## 5. Notation

| | | |
|---|---|---|
| $A$ | $[\mathrm{m}^2]$ | Area |
| $\mathbf{c}$ | $[\frac{\mathrm{mol}}{\mathrm{m}^3}]$ | Concentration of reactive species |
| $c_s$ | $[\frac{1}{\mathrm{s}}]$ | Collision rate factor |
| $c_{\Delta\wp_{ij}}$ | $[\mathrm{kg}]$ | Momentum exchange factor |
| $\mathbf{D}$ | $[\frac{\mathrm{s}}{\mathrm{m}^2}]$ | Dusty-Gas Matrix of diffusivities |
| $\mathbf{D}^a_{eff}$ | $[\frac{\mathrm{m}^2}{\mathrm{s}}]$ | Matrix of diffusivities within the active phase |
| $\mathbf{D}^S$ | $[\frac{\mathrm{m}^2}{\mathrm{s}}]$ | Matrix of surface diffusivities |
| $D_{ij}$ | $[\frac{\mathrm{m}^2}{\mathrm{s}}]$ | Binary diffusivity |
| $d$ | $[\mathrm{m}]$ | Diameter |
| $\mathbf{e}$ | $[-]$ | Vector having all elements 1 |
| $F$ | $[\mathrm{N}]$ | Force |
| $\mathbf{j}$ | $[\frac{\mathrm{mol}}{\mathrm{m}^2\mathrm{s}}]$ | Mole flux |
| $k$ | $[\frac{1}{\mathrm{s}}]$ | Reaction rate constant |
| $\mathbf{k}_S$ | $[\frac{\mathrm{m}}{\mathrm{s}}]$ | Mass-transfer coefficients |
| $M$ | $[\frac{\mathrm{kg}}{\mathrm{kmol}}]$ | Molecular weight |
| $m_r$ | $[\mathrm{kg}]$ | Reduced mass |
| $N$ | $[-]$ | Number of species |
| $n$ | $[-]$ | Number of particles |
| $n_r$ | $[-]$ | Number of chemical reactions |
| $p$ | $[\mathrm{Pa}]$ | Pressure |
| $p_i$ | $[\mathrm{Pa}]$ | Partial pressure |
| $\wp$ | $[\frac{\mathrm{N \cdot m}}{\mathrm{s}}]$ | Momentum |
| $R$ | $[\frac{\mathrm{J}}{\mathrm{mol\ K}}]$ | Gas constant |

| | | |
|---|---|---|
| $R_i$ | $[\frac{\mathrm{mol}}{\mathrm{m^3 \cdot s}}]$ | Reaction rate |
| $R_0$ | $[\mathrm{m}]$ | Radius of composite particle |
| $r$ | $[\mathrm{m}]$ | Radius |
| $r_{exp}$ | $[\frac{\mathrm{mol}}{\mathrm{m^3 s}}]$ | Experimental reaction rate |
| $r_{int}$ | $[\frac{\mathrm{mol}}{\mathrm{m^3 s}}]$ | Intrinsic reaction rate |
| $r_P$ | $[\mathrm{m}]$ | Average pore radius |
| $s$ | $[\frac{1}{\mathrm{s}}]$ | Collision rate of particles |
| $Re$ | $[-]$ | Reynolds number |
| $Sc$ | $[-]$ | Schmidt number |
| $Sh$ | $[-]$ | Sherwood number |
| $T$ | $[K]$ | Temperature |
| $t$ | $[\mathrm{s}]$ | Time |
| $u$ | $[\frac{\mathrm{m}}{\mathrm{s}}]$ | Velocity |
| $u_r$ | $[\frac{\mathrm{m}}{\mathrm{s}}]$ | Relative velocity |
| $V$ | $[\mathrm{m}^3]$ | Volume |
| $x$ | $[-]$ | Volume fraction |
| $z$ | $[\mathrm{m}]$ | Direction |

### Greek symbols

| | | |
|---|---|---|
| $\epsilon$ | $[-]$ | Porosity |
| $\zeta$ | $[-]$ | Volume fraction of the active component |
| $\eta$ | $[\mathrm{Pas}]$ | Viscosity |
| $\nu$ | $[-]$ | Vector of stoichiometric co-efficients |
| $\nu$ | $[-]$ | Diffusion volume (Fuller *Eq.* only) |
| $\sigma$ | $[\mathrm{m}^2]$ | Cross section |
| $\tau$ | $[-]$ | Tortuosity |
| $\Phi$ | $[-]$ | Thiele modulus |
| $\varphi$ | $[-]$ | Effectiveness factor |
| $\chi$ | $[-]$ | Deflection angle |
| $\nabla$ | $[-]$ | Gradient operator |

### Indices

| | |
|---|---|
| $a$ | Active phase |
| $b$ | Bulk phase |
| $D$ | By diffusion |
| $eff$ | Effective |
| $exp$ | Experimental |
| $i, j, l$ | Species index |
| $i_r$ | Reaction index |
| $int$ | Intrinsic |
| $K$ | Knudsen |
| $M$ | Momentum exchange |
| $m$ | Matrix phase |

| | |
|---|---|
| $r$ | Reactor |
| $S$ | Surface |
| $t$ | Total |
| $V$ | Viscous flux |

## Acknowledgement

This work was financially supported by the Max-Büchner Forschungsstiftung and Fonds der Chemischen Industrie.

## References

BIRD, G. A. (1994): Molecular Gas Dynamics and the Direct Simulation of Gas Flows, Oxford, Clarendon Press, pp. 38–69.

BRAUER, H. (1971): Stoffaustausch einschliesslich chemischer Reaktionen (Mass-Transfer Including Reactions), Aarau, Frankfurt a. M., Verlag Sauerlaender, p. 483 (in German).

CHAPMAN, C. (1917): On the Kinetic Theory of a Gas: Part II – A Composite Monoatomatic Gas: Diffusion, Viscosity, and Thermal Conduction, *Phil. Trans. Roy. Soc.*, Vol. 217, pp. 115–197.

FENG, C. F. (1972): Multicomponent Gaseous Diffusion and Flow Through Catalyst Particles, PhD Thesis, Univ. of Wisconsin, Dept. of Chemical Engineering.

FULLER, E. N. – SCHETTLER, P. D. – GIDDINGS, J. C. (1966): *Ind. Eng. Chem.*, Vol. 58, No. 5, p. 18.

HINDERER, J. – KEIL, F. J. (1994): Monte-Carlo Calculations: Diffusion in Zeolites, *Periodica Polytechnica Ser. Chem. Eng.*, Vol. 38, pp. 75–80.

HINDERER, J. – KEIL, F. J. (1995): Diffusion and Reaction in Composite Catalysts, *Hung. J. Ind. Chem.*, Vol. 23, pp. 207–213.

HINDERER, J. – KEIL, F. J. (1996): Three-Dimensional Monte-Carlo Calculations of Diffusion and Reaction Phenomena in Zeolites, *Chem. Eng. Sci.*, Vol. 51, pp. 2667–2672.

ESPIONZA, R. L. – STANDER, C. M. – MANDERSLOOT, W. G. B. (1983): Catalytic Conversion of Methanol to Hydrocarbons over Amorphous or Zeolite Silica-Alumina, *Appl. Catal.*, Vol. 6, pp. 11–26.

KRISHNA, R. (1993): A Unified Approach to the Modelling of Intraparticle Diffusion in Adsorption Processes, *Gas Sep. Purif.*, Vol. 7, No. 2, pp. 91–104.

MARTIN, H. (1988): Low Peclet Number Particle-To-Fluid Heat and Mass Transfer in Packed Beds, *Chem. Eng. Sci.*, Vol. 33, pp. 913–919.

RIECKMANN, C. – KEIL, F. J.(1997): Multicomponent Diffusion and Reaction in Three-Dimensional Networks - General Kinetics, submitted to *Ind. Eng. Chem. Res.*

RUCKENSTEIN, E. (1970): The Effectiveness of Diluted Porous Catalysts, *AIChE J.*, Vol. 16, No. 1, pp. 151–153.

SCHOENFELDER, H. – HINDERER, J. – WERTHER, J. – KEIL, F. J. (1994): Methanol to Olefins - Prediction of the Performance of a Circulating Fluidized-Bed Reactor on the Basis of Kinetic Experiments in a Fixed-Bed Reactor, *Chem. Eng. Sci.*, Vol.49, No. 24B, pp. 5377–5390.

THIELE, E. W. (1939): Relation between Catalytic Activity and Size of Particle, *Ing. Engng. Chem.*, Vol. 31, No. 7, pp. 916–920.